mAbs 5:1, 1–14; January/February 2013; © 2013 Landes Bioscience

Adsorption behavior of a human monoclonal antibody at hydrophilic and hydrophobic surfaces

Ruairidh G. Couston,[1] Maximilian W. Skoda,[2] Shahid Uddin[3] and Christopher F. van der Walle[1,†,*]

[1]Strathclyde Institute of Pharmacy and Biomedical Sciences; University of Strathclyde; Glasgow, Scotland, UK; [2]STFC; Rutherford Appleton Laboratory; Harwell; Didcot, Oxford, UK; [3]MedImmune Ltd.; Formulation Sciences; Biopharmaceutical Development; Aaron Klug Building; Granta Park, Cambridge, UK

[†]Current Address: MedImmune Ltd.; Formulation Sciences; Biopharmaceutical Development; Aaron Klug Building; Granta Park, Cambridge, UK

Keywords: mAb, interface, desorption, polysorbate, neutron reflectometry, self assembled monolayer

One aspiration for the formulation of human monoclonal antibodies (mAb) is to reach high solution concentrations without compromising stability. Protein surface activity leading to instability is well known, but our understanding of mAb adsorption to the solid-liquid interface in relevant pH and surfactant conditions is incomplete. To investigate these conditions, we used total internal reflection fluorescence (TIRF) and neutron reflectometry (NR). The mAb tested ("mAb-1") showed highest surface loading to silica at pH 7.4 (~12 mg/m^2), with lower surface loading at pH 5.5 (~5.5 mg/m^2, further from its pI of 8.99) and to hydrophobized silica (~2 mg/m^2). The extent of desorption of mAb-1 from silica or hydrophobized silica was related to the relative affinity of polysorbate 20 or 80 for the same surface. mAb-1 adsorbed to silica on co-injection with polysorbate (above its critical micelle concentration) and also to silica pre-coated with polysorbate. A bilayer model was developed from NR data for mAb-1 at concentrations of 50–5000 mg/L, pH 5.5, and 50–2000 mg/L, pH 7.4. The inner mAb-1 layer was adsorbed to the SiO_2 surface at near saturation with an "end-on" orientation, while the outer mAb-1 layer was sparse and molecules had a "side-on" orientation. A non-uniform triple layer was observed at 5000 mg/L, pH 7.4, suggesting mAb-1 adsorbed to the SiO_2 surface as oligomers at this concentration and pH. mAb-1 adsorbed as a sparse monolayer to hydrophobized silica, with a layer thickness increasing with bulk concentration - suggesting a near end-on orientation without observable relaxation-unfolding.

Introduction

Therapeutic antibodies are used to treat a wide variety of conditions and their value to the pharmaceutical industry is increasing.[1] When administered via low volume subcutaneous injection, there is a general requirement for high concentration liquid formulation to achieve the therapeutic dose. Proteins formulated as high concentration liquids are susceptible to aggregation through a number of destabilization mechanisms,[2] one including surface adsorption-desorption, which has been the subject of review.[3] Misfolded protein may reveal hydrophobic residues that facilitate protein aggregation through hydrophobic interactions. These interactions may lead to formation of soluble aggregates (oligomers), which in turn may nucleate further protein aggregation, ultimately generating visible particles in solution.[4,5] The pharmacopeias state that particles > 10 μm and 25 μm should remain below 6000 and 600 particles/container, respectively, and that measurement can be made by light obscuration (USP < 788 > and EP 2.9.19). There is considerable discussion in the industry around the characterization of protein aggregation and particulates and how this information can be used with regard to understanding the potential capacity of particulates to elicit immunogenic responses.[6-8]

Excipients are often included in protein formulations to stabilize the monomeric form and reduce aggregation and surface adsorption.[9] Many examples can be drawn on to illustrate the utility of polysorbates in protein bioprocessing, formulation and delivery. In general, polysorbates compete with the protein for an interface and adsorb to exposed hydrophobic patches on the protein surface. Non-ionic surfactants such as polysorbate 20 and 80 (Tween® 20 and 80) and the polyethylene glycol-polypropylene glycol-polyethylene glycol (PEO-PPO-PEO) triblock co-polymers (Pluronics®) are commonly used excipients for this reason.[10,11] Tweens around 0.02–0.05% are often found to minimize particulate formation during shaking/stirring formulation studies designed to expose the protein to air/liquid interfaces and accelerate aggregation through surface adsorption/desorption. However, while aggregates ≥ 10 μm and ≥ 25 μm in size may be attenuated, particles toward the subvisible may still be present.[12] Low concentrations of Tween 20 (0.0025%, below the critical micelle concentration (CMC) of *ca*. 0.01% w/v) may also confer some prevention of IgG1 aggregation when shaken.[12] Tween 20 has also been shown to displace β-lactoglobulin from the air/water interface by preferential adsorption,[13] and aggregation of recombinant human factor XIII by competition for interfacial binding sites.[14]

*Correspondence to: Christopher F. van der Walle; Email: wallec@medimmune.com
Submitted: 09/03/12; Revised: 10/09/12; Accepted: 10/10/12
http://dx.doi.org/10.4161/mabs.22522

This manuscript has been published online, prior to printing. Once the issue is complete and page numbers have been assigned, the citation will change accordingly.

©2012 Landes Bioscience. Do not distribute.

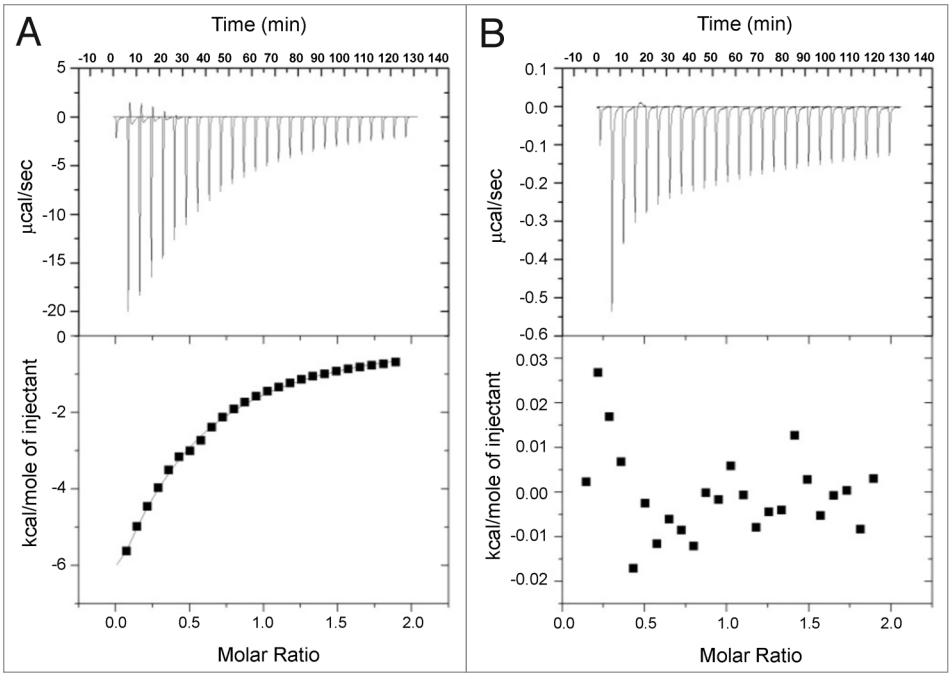

Figure 1. Enthalpograms for the titration of 10 mM Tween 80 into 14.4 mg/mL (0.24 mM) BSA (A), and 10 mM Tween 80 into 14.4 mg/mL mAb-1 (B). Top panels show power flow signals for each injection of polysorbate into the protein solution. Bottom panels show the reaction enthalpies as determined by peak integration.

Loss of protein at the solid/liquid interface is also an important consideration and may be particularly relevant during dilution and administration that involve use of plastic bags and intravenous lines.[15] Adsorption of mAbs to glass vials has been shown to be due predominantly to electrostatic interactions.[16] Protein relaxation at the solid/liquid interface generally refers to an unfolding event for the adsorbed protein and concomitant increase in its footprint. One report has shown that the protein footprint may increase 5-fold during relaxation on hydrophobic surfaces, though much less so on hydrophilic surfaces and with longer time scales.[17] It is not always the case, however, that proteins unfold on hydrophobic surfaces. This may be related to the conformational stability of the protein and, for mAbs at least, there are recent reports that adsorption to hydrophobic surfaces is not necessarily followed by unfolding.[18,19] The influence of polysorbate on adsorbed protein is by conventional wisdom one where surfactant desorbs protein from an interface in a process sometimes referred to as orogenic displacement.[20,21] Polysorbates, however, may be co-added to a liquid protein formulation or used to pre-coat a glass vial before filling; both scenarios are very different to displacement studies. In these scenarios, polysorbate has been shown to have no effect on protein adsorption, particularly at glass surfaces where the polysorbate-silica interaction is relatively weak.[22]

Here, we report results of our investigation of the adsorption and desorption of a human monoclonal antibody at the solid/water interface, initially using total internal reflection fluorescence (TIRF).[23,24] TIRF is dependent on the generation of an evanescent wave at the point of total internal reflection that excites fluorophores within *ca*. 100 nm of the surface (dependent on the wavelength), i.e., the emission signal is generated by excitation of (fluorescently labeled) protein adsorbed at the solid/liquid interface and not from protein in solution.[25] For transport limited adsorption, as described by the Leveque equation, the raw fluorescent signal can be converted to a quantitative measure of mass per unit area. In this manner TIRF is a relatively straightforward bench-top technique allowing determination of adsorption/desorption kinetics for a fluorescently labeled protein at the solid/liquid interface; however, transport limited kinetics are only maintained for low protein concentrations and TIRF does not provide molecular-level information of the nature of the adsorbed protein layer, such as orientation of the protein molecules at the surface, and the build-up of multiple protein layers. To ascertain this information for protein adsorbed from relatively high concentration solutions, we characterized the adsorbed protein layers using neutron reflectometry (NR, a general technique described elsewhere[26]) NR has been used to define the orientation of antibodies non-specifically adsorbed at the solid/liquid interface[19] and antibodies non-covalently bound at surfaces engineered to harbor specific capture ligands.[27] By analyzing data generated by TIRF and NR experiments, we describe the differential adsorption/desorption of a human monoclonal antibody at silica and alkyl-silanized silica surfaces from aqueous solution of varying pH in the presence and absence of polysorbate 20/80 above and below their CMC.

Results

Confirmation of transport limited surface adsorption for mAb-1. For the TIRF experiments, it was important to establish that transport to the surface was not driven by the fluorophore or in the case of pre-injection with Tween, direct binding of mAb-1 to the surfactant. No fluorescence signal above the background for buffer alone was observed upon injection of fluorescein isothiocyanate (FITC) or Alexa Fluor 488 5-SDP (null data not shown). Isothermal titration calorimetric (ITC) data demonstrated that there was no specific binding between mAb-1 and either Tween 20 or 80, in contrast to the positive control, which was bovine serum albumin (BSA) binding to Tween 20 with a K_a of $4.02 \times 10^3 \pm 565$ M^{-1} for a one-site binding model (Fig. 1) and to Tween 80 with a K_a of $1.32 \times 10^2 \pm 78.9$ M^{-1} (data very similar to Tween 20). These calorimetry results are consistent with previous reports for titration of polysorbate against three other mAbs and albumin in solution.[28]

©2012 Landes Bioscience. Do not distribute.

The fluorescein-labeled mAb-1 was diluted in phosphate buffered saline (PBS), pH 7.4, when carrying out the TIRF experiments since fluorescein fluorescence is attenuated in mildly acidic conditions.[29] For the same reason we used Alexa Fluor 488 label when carrying out TIRF experiments at pH 5.5. The Leveque equation (Eq. 1) was used to establish that mAb-1 surface adsorption was transport limited (below), such that the raw fluorescence data were fitted to the equation to calculate the protein surface fraction in units of mg/m^2.

$$\frac{d\Gamma}{dt} = 0.538 \cdot \left(\frac{\gamma}{L}\right)^{\frac{1}{3}} \cdot D^{\frac{2}{3}} \cdot C$$

where, $d\Gamma/dt$ = adsorption rate; γ = shear rate; L = distance from point of entry to measurement point (cm); D = diffusion coefficient (calculated as 1.99×10^{-10} for a measured hydrodynamic diameter of 12.17 nm) and; C = concentration (mg/mL).[30]

The two parameters in the Leveque equation that could be varied in these experiments were shear rate (γ) and concentration (C), the other parameters remaining constant. To establish transport limited adsorption, we therefore calculated the change in the rate of adsorption (i.e., the linear slope of fluorescence vs time) for increasing concentrations of mAb-1 (maintaining shear at 6 sec^{-1}), and increasing shear (for L = 1 cm and a mAb-1 concentration of 0.01 mg/mL). Plots in Figure 2 showed that the change in the rate of adsorption was directly proportional to the mAb-1 concentration and also proportional to the cube root of shear (as predicted by the Leveque equation), and therefore demonstrating that transport limited conditions were maintained up to a maximum concentration of 250 mg/L and maximum shear rate of 42 sec^{-1}.

Polysorbate-induced desorption of mAb-1 from silica surfaces. Desorption of mAb-1 from the silica surface at pH 7.4 by both Tween 20 and 80 at concentrations below and above their CMC was observed (Fig. 3). Good reproducibility for the TIRF technique in measuring mAb-1 behavior at the surface was demonstrated by overlap of the profiles representing the adsorption phase (i.e., to the point of polysorbate injection), although the profile for 1 mM Tween 80 appeared to be slightly displaced upward. Displacement of mAb-1 from the surface was rapid and near complete for injection of Tween 20 both below and above its CMC: ~1 mg/m^2 mAb-1 remaining compared with ~12 mg/m^2 for mAb-1 under equilibrium conditions (at the plateau in the absence of surfactant). In contrast, much less mAb-1 was desorbed from the surface by Tween 80 below and above its CMC (*ca.* 7 and 2 mg/m^2 remaining adsorbed, respectively). The kinetics of mAb-1 desorption were also very slow for Tween 80 below its CMC. With respect to the extent of mAb-1 desorption, the affinity of Tween 20 for the silica surface was therefore greater than that for Tween 80.

Co-injection of polysorbate and mAb-1 to the silica surface. The concentration of Tween co-injected with mAb-1 into the sample chamber had a distinct influence on mAb-1 surface adsorption (Fig. 4). When co-dissolved at concentrations above their CMCs both polysorbates increased mAb-1 surface adsorption to a similar degree – when measured at the plateau near steady-state conditions (~25–30 mg/m^2) and relative to mAb-1 in the absence of polysorbate (~12 mg/m^2). There was no discernible change in the rate of adsorption from the point of

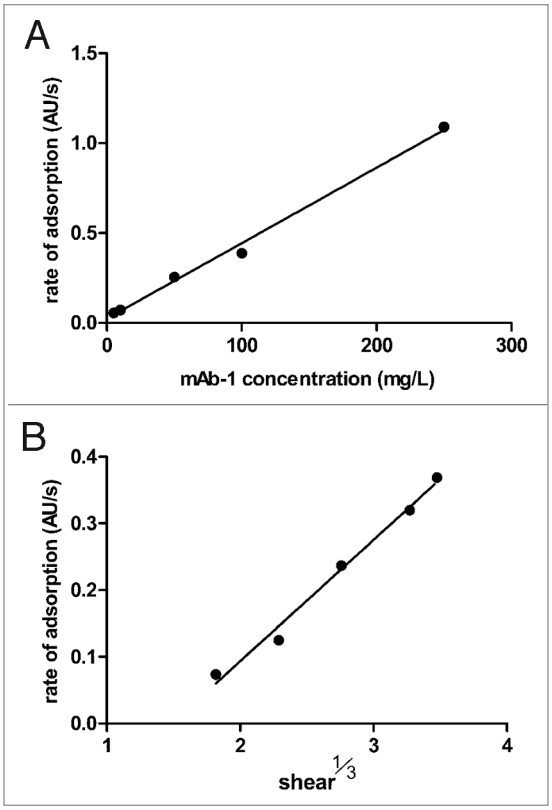

Figure 2. TIRF data showing linear relationships for the rate of adsorption of mAb-1 to the glass surface vs. its concentration for a constant shear of 6 sec^{-1} (A), and the cube root of the shear rate for a mAb-1 concentration of 0.01 mg/mL (B), according to the Leveque equation.

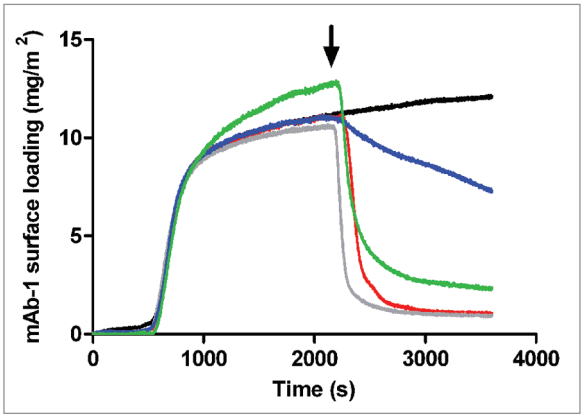

Figure 3. Adsorption of a 0.01 mg/mL solution of mAb-1 to a glass surface (black line), investigated using TIRF, followed by introduction of polysorbate (arrow) in PBS pH 7.4 as follows: Tween 20, 0.05 mM (red line) and 1 mM (gray line); Tween 80, 5 μM (blue line) and 1 mM (green line).

©2012 Landes Bioscience. Do not distribute.

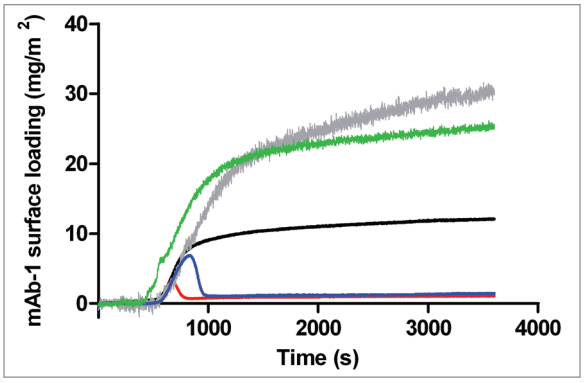

Figure 4. Adsorption of a 0.01 mg/mL solution of mAb-1 co-dissolved with polysorbate to a glass surface in PBS pH 7.4, investigated using TIRF, as follows: Tween 20, 0.05 mM (red line) and 1 mM (gray line); Tween 80, 5 μM (blue line) and 1 mM (green line). Reference was to the adsorption of a 0.01 mg/mL solution of mAb-1 to a glass surface (black line).

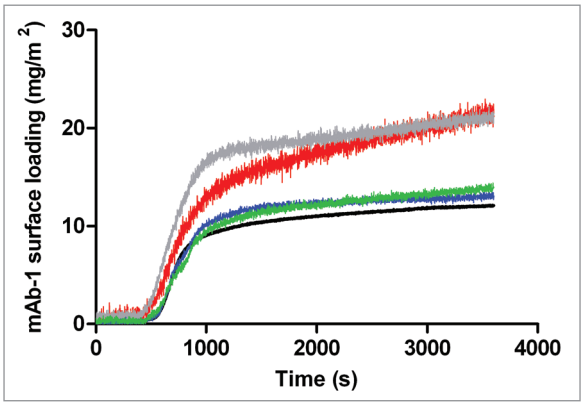

Figure 5. Adsorption of a 0.01 mg/mL solution of mAb-1 to a glass surface pre-coated with polysorbate in PBS buffer pH 7.4, investigated using TIRF, as follows: Tween 20, 0.05 mM (red line) and 1 mM (gray line); Tween 80, 5 μM (blue line) and 1 mM (green line). Reference was to the adsorption of a 0.01 mg/mL solution of mAb-1 to a glass surface (black line).

injection of sample. It is also noticeable that the TIRF signals for mAb-1 co-dissolved with Tween 20/80 above their CMCs were relatively noisy. It is not entirely clear why this should be, but may point to a large degree of change of mAb-1 approaching and leaving a surface. That is, the surface is not to be assumed to be a static layer but one that is under a degree of flux consistent with competition for the surface between surfactant and protein. In contrast, co-injection of mAb-1 with Tween 20 or 80 below their CMCs resulted in a marked decrease in surface adsorption (Fig. 4). This suggests that saturation by polysorbate of non-specific binding sites on mAb-1, and polysorbate directed adsorption under these specific conditions, is important in understanding the observed switch from increased mAb-1 adsorption to desorption. The transient peak indicates that mAb-1 initially absorbed to the silica surface but was then competed off the surface by both Tween 20 and Tween 80 as equilibrium conditions became established. The transient peak for mAb-1 co-injection with 5 μM Tween 80 was larger than for co-injection with 50 μM Tween 20. This can most likely be attributed to the 10-fold lower concentration (compare Tween 20) or the lower affinity of Tween 80 for the silica surface compared with Tween 20, consistent with the observations made for desorption of mAb-1 by the two polysorbates below their CMCs.

Adsorption of mAb-1 to silica surfaces pre-coated with polysorbate. To further investigate the apparent competition between the mAb-1 and polysorbate for the silica surface, we pre-injected Tween 20 and 80 onto the surface for 1800 sec without mAb-1. The expectation was that the surface would become coated with either Tween 20 or 80 to a saturation dependent on the polysorbate's affinity for the silica surface. mAb-1 solution without polysorbate was then injected into the sample chamber as normal (Fig. 5). For Tween 80, the extent of adsorption of mAb-1 at near plateau was approximately equivalent to that for mAb-1 at the bare silica surface (*ca*. 12–14 mg/m^2 for Tween 80 coated surfaces). For pre-coating with Tween 20, a much higher subsequent adsorption of mAb-1 was observed (~20 mg/m^2). This suggests that Tween 80 adsorbed poorly to the surface, while the affinity of Tween 20 for the surface was greater, which is consistent with interpretations above. The data suggest that mAb-1 does not displace Tween 20 from the silica surface, else the profiles would have tended to that for adsorption to silica. There was no significant difference between mAb-1 adsorbed to surfaces pre-coated with polysorbate above or below its CMC because the surfactants were injected over a sustained period of time (i.e., to saturation), with the remaining bulk solution then washed out on injection of mAb-1.

The effect of solution pH on mAb-1 adsorption. The pI of mAb-1 was given as 8.99 and its adsorption to the silica surface from solutions at pH 5.5 and pH 7.4 were investigated because electrostatic interaction between a protein and the surface is known to play a central role in driving adsorption.[31] Figure 6 shows that mAb-1 surface adsorption at pH 7.4 was approximately three times that at pH 5.5 (ca. 12 mg/m^2 compared with *ca*. 5.5 mg/m^2, respectively). At both pH values, mAb-1 would be expected to carry a net positive charge facilitating electrostatic attraction with the net negatively charged silica surface. The difference in surface adsorption may therefore arise from subtle changes in the charged state of local patches of acidic/basic residues; this was further investigated by neutron reflectivity measurements as described below. The acid sensitivity of Alexa Fluor 488, however, cannot be discounted (though it is much more stable than fluorescein). The manufacturer states a stable pH range of 4–10 but recommends a useable pH range of 6.5 to 8.5, which is outside the pH studied here. Explaining the apparent fall in surface adsorption is thus complicated by a possible decrease in fluorescence sensitivity at pH 5.5.

mAb-1 adsorption and desorption from hydrophobic surfaces. To mimic hydrophobic plastic surfaces, we silanized silica with octadecyltrichlorosilane (OTS) to generate octadecyl monolayer.[32] The water contact angle of the OTS-coated silica surface was 107.1°, which indicated a poorly wettable (i.e., hydrophobic) surface. This compared against a water contact angle of

©2012 Landes Bioscience. Do not distribute.

51.2° for the bare silica surface (i.e., hydrophilic). The amount of mAb-1 adsorbed to the OTS-coated surface was around half that adsorbed to bare silica and was reduced compared with the hydrophilic silica surface (Fig. 6). This would imply a reduced number of molecules bound per unit area to the OTS-coated surface, though the TIRF data does not inform us of layer thickness. We therefore characterized the nature of the adsorbed layer using neutron reflectivity. Injection of Tween 20 or 80 caused an initial period of rapid desorption of mAb-1 from the OTS-coated surface whether the concentrations of polysorbate were above and below their CMC values (Fig. 7). Desorption of mAb-1 by Tween 80 rapidly reached a nadir with little or no further desorption, leaving around 40% of the mAb-1 originally adsorbed. In contrast, desorption by Tween 20 was not complete at the end of the data collection period. This result is opposite to that seen for mAb-1 desorption from bare silica, where Tween 20 caused greater, more rapid desorption than Tween 80. This supports the same interpretation that the relative affinity of the polysorbate determines the extent to which mAb-1 is desorbed.

It should be noted that there appeared to be a greater variability in the extent of adsorption of mAb-1 to the OTS-coated surface in Figure 7. This probably reflects subtle differences in the quality of the octadecyl surface for the different coated substrates. It is well known that imperfections in alkyl self-assembled monolayers are largely eliminated when the silanization is allowed to proceed for extended periods (e.g., overnight), but surface consistency for the OTS-coated glass slides would naturally be expected to be lesser compared with the bare, cleaned glass slides. A further consideration is the change in scale of the y-axis, given that much smaller amounts of mAb-1 adsorb to the OTS-coated surface compared with bare silica.

For hydrophobic silica surfaces pre-coated with polysorbate, mAb-1 adsorption appeared to be dependent on the prior concentration of polysorbate used to coat the surface (Fig. 8). However, it should be noted that the absolute change in surface loading remained small for all pre-coating conditions tested, as discussed further below.

Characterization of the protein surface fraction and antibody orientation within adsorbed layer(s). It became apparent during the course of the TIRF experiments that interpretation of the data would be aided by a better understanding of the nature of the adsorbed mAb-1 layer(s) to silica and OTS-coated silica. Neutron reflectivity experiments were therefore used to generate a model of how mAb-1 may adsorb to the various surfaces during change in concentration and pH. On fitting parameters to the data for the protein in D_2O, it was found that the best agreement (as measured by χ^2) was only achievable when the scattering length density (SLD) for the protein layer was allowed to become less than the theoretical value calculated for 70% hydrogen/deuterium (H/D) exchange. This would infer a protein layer with a surface fraction of > 1.0, which is unphysical. Since the data fitting appeared to point toward a saturated layer (i.e., mAb-1 surface fraction of 1.0) we therefore calculated the theoretical SLD against the data fitting that was equivalent to an assumed H/D exchange of 50%. This gave a revised theoretical SLD of 2.57×10^{-6} Å^{-2} against which all other protein surface fractions

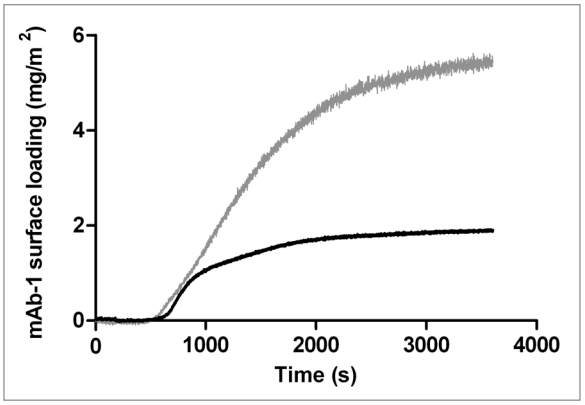

Figure 6. Adsorption of a 0.01 mg/mL solution of mAb-1 histidine buffer pH 5.5 to a glass surface (gray line) and to an OTS-coated (hydrophobized) glass surface (black line), investigated using TIRF.

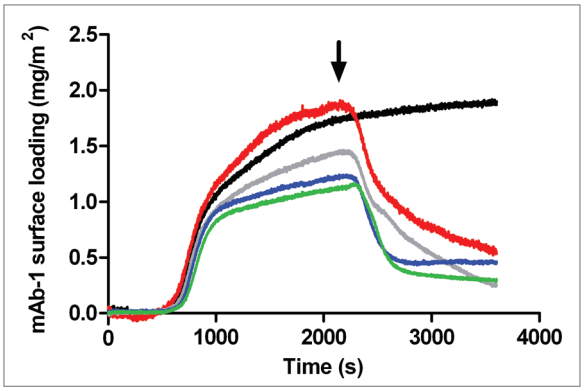

Figure 7. Adsorption of a 0.01 mg/mL solution of mAb-1 to an OTS-coated glass surface (black line), investigated using TIRF, followed by introduction polysorbate (arrow) in histidine buffer pH 5.5 as follows: Tween 20, 0.05 mM (red line) and 1 mM (gray line); Tween 80, 5 μM (blue line) and 1 mM (green line).

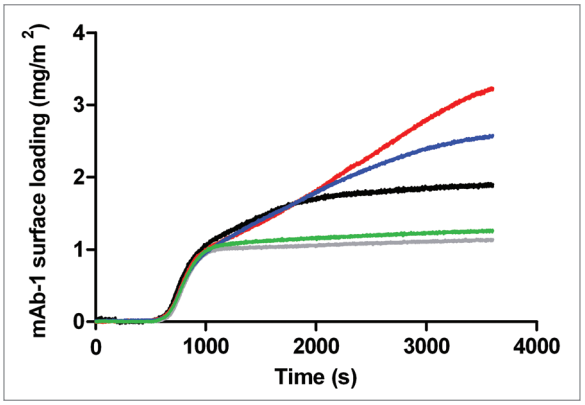

Figure 8. Adsorption of a 0.01 mg/mL solution of mAb-1 to an OTS-coated glass surface pre-coated with polysorbate in histidine buffer pH 5.5, investigated using TIRF, as follows: Tween 20, 0.05 mM (red line) and 1 mM (gray line); Tween 80, 5 μM (blue line) and 1 mM (green line). Referenced to the adsorption of a 0.01 mg/mL solution of mAb-1 to a OTS-coated glass surface (black line).

©2012 Landes Bioscience. Do not distribute.

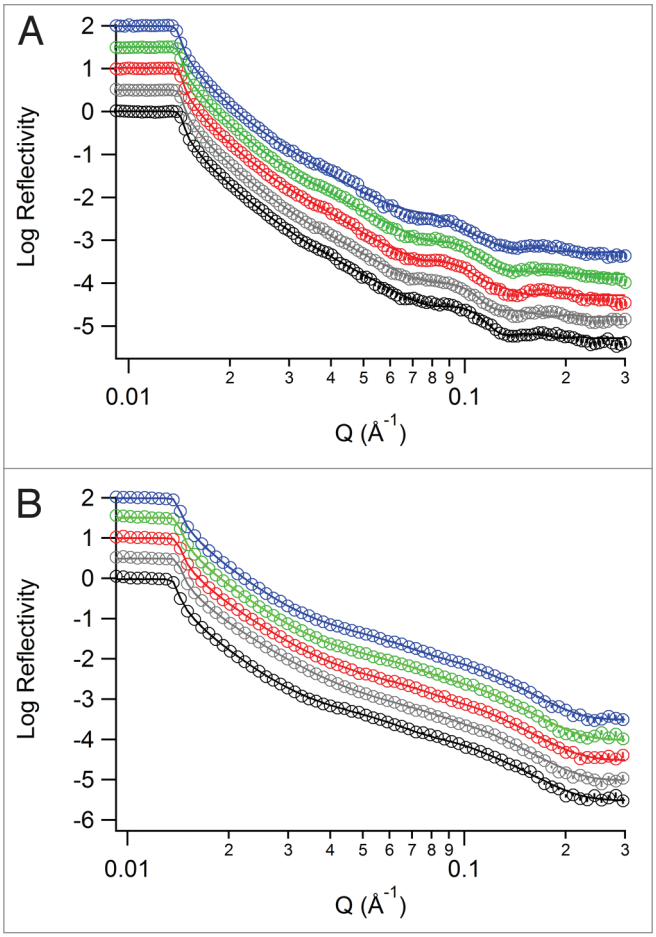

Figure 9. Neutron reflectivity profiles for mAb-1 adsorbed to a SiO_2 (A) and OTS-coated SiO_2 (B) surface at bulk concentrations of 50 (black), 200 (gray), 500 (red), 2000 (green) and 5000 (blue) mg/ml in histidine buffer pH 5.5. Data points are shown as empty circles, with the fitted reflectivity profiles shown as solid lines in the same color. For clarity, reflectivity profiles for increasing bulk concentrations are sequentially offset in the ordinate by a factor of $\log_{10}0.5$.

were calculated (using Equation 3 in Materials and Methods). Although the percentage H/D exchange is lower than values typically assumed, this may not in fact be unreasonable. Given a saturated surface with a fully packed protein layer, neighboring mAb-1 molecules would minimize exposure of the molecular surface exposed to the solvent and consequently H/D exchange. This would be consistent with the known reduction in the rate of H/D exchange for lysozyme adsorbed to the silica surface compared with lysozyme in bulk solution.[33]

While TIRF necessarily required very low concentrations to obey Leveque conditions, there is no such requirement for analysis of steady-state adsorption by NR; since the NR experiments were intended to capture the molecular nature of the adsorbed layers after ~30 min equilibration. The range of concentrations under which mAb-1 was adsorbed to surfaces represented concentrations that may reasonably be encountered during early formulation development. Practicality of available mAb-1 vs. the required sample size did, however, limit the bulk concentration to a maximum of 5 mg/mL, less than the highest concentrations which monoclonal antibodies are commonly concentrated to for subcutaneous injection (ca. 50–150 mg/mL). Nevertheless, over all concentrations tested, the adsorption of mAb-1 to hydrophilic surfaces (SiO_2—equivalent to the bare silica slides used in TIRF experiments) and hydrophobic surfaces (OTS-coated SiO_2) was clearly distinguished. The reflectivity profiles for mAb-1 adsorbed to SiO_2 from pH 5.5 buffer (Fig. 9A) show a clear fringe at Q of 0.09 Å^{-1} with neighboring fringes at higher and lower Q values (the latter being rather shallow). In contrast, reflectivity profiles for mAb-1 adsorbed to OTS-coated SiO_2 from pH 5.5 buffer show only a single, broad fringe at Q of 0.1 Å^{-1} (Fig. 9B). This pattern of fringes was repeated for all concentrations tested and suggests the formation of additional layers for mAb-1 absorbed to SiO_2. On fitting the SLD profiles to these data sets (Fig. 10), the OTS-coating was observed as a 17 Å layer with a negative SLD of ~0.76×10^{-6} Å^{-2}, which is very similar to parameters previously fitted by others for an OTS layer to SiO_2 (thickness of 16 Å and SLD $-0.5 \pm 0.3 \times 10^{-6}$ Å^{-2}).[34] Progressing from concentrations of 50 mg/L to 5000 mg/L saw a transition in the SLD profile to higher protein surface fraction with a concomitant increase in the layer thickness (**Table 1**). Together, these transitions suggest a reorientation of a single mAb-1 layer at the hydrophobic surface as the absorbed population increases. N-sigma analysis[35] for 1-layer and 2-layer protein models at the OTS-coated surface statistically favored the protein monolayer, and this is consistent with the smaller χ^2 values.

Fitting of the SLD profile of the bare SiO_2 layers benefitted (in terms of χ^2 values) from the addition of a very thin layer, 1.5 to 3.5 Å with SLD 0.35 to 0.61×10^{-6} Å^{-2}, suggestive of a very sparse hydrogenous layer that presumably remained following the cleaning process. This sparse hydrogenous layer did not appear to subsequently direct mAb-1 adsorption since distinct profiles were observed from bulk solutions of differing pH. At both pH 5.5 and 7.4 for concentrations up to 2000 mg/L, the fitted SLD profiles showed a mAb-1 bilayer (Fig. 10), with N-sigma analysis for bilayer and trilayer models also being statistically in favor of a bilayer. The SLD profiles further showed that the orientation and surface fraction of both mAb-1 layers was strongly dependent on both pH and concentration. At pH 7.4, the thickness of the layer immediately adsorbed to the SiO_2 layer (the "inner layer") progressively increased from ~130 to 150 Å with increasing bulk concentration (**Table 1**). Most dramatic, however, was the reorientation of the mAb-1 molecules within the "outer layer" (mAb-1 adsorbed to the inner layer) at pH 7.4. At bulk concentrations of 5000 mg/l, a sparse additional outer layer emerges, with the mAb-1 molecules adsorbed end-on in all three layers at this concentration. The strong propensity for mAb-1 to be oriented end-on at pH 7.4 is expected to decrease the protein surface fraction (for the same number of molecules per unit area) since the footprint is smaller end-on than side-on. Conversely, a small increase in the protein surface fraction of the inner and outer layers is observed on increasing the concentration from 2000 to 5000 mg/L, pH 7.4. This implies that a significant number of additional mAb-1 molecules adsorbed during transition from bilayer to trilayer over these concentrations. Adsorption of mAb-1 from pH 5.5 buffer was distinct from adsorption from pH 7.4 buffer in

©2012 Landes Bioscience. Do not distribute.

three keys areas: (1) the protein surface fraction of the inner layer was slightly higher and did not show a clear, progressive increase with increasing bulk concentration; (2) the thickness of the inner layer at concentrations to 200 mg/L suggested a greater propensity for side-on orientation; and (3) no dramatic reorientation was observed for the outer layer for adsorption from 5000 mg/L concentrations. Similar to adsorption from pH 7.4, the surface fraction of the outer mAb-1 layer remained sparse (SLD around 5.5×10^{-6} Å^{-2}), which was also equivalent to the surface fraction of mAb-1 adsorbed to OTS-coated silica.

Discussion

The influence of polysorbate on mAb-1 adsorption to silica. Three conditions were tested: pre-, co- and post-injection of polysorbate with respect to the point of mAb-1 injection to the surface. Both Tween 20 and 80 caused desorption of mAb-1 from the silica surface dependent on their relative affinities for the surface and concentration. The longer C18 alkyl-chain of Tween 80 would be expected to reduce its affinity for the hydrophilic silica surface compared with the C12 alkyl-chain of Tween 20, with the opposite being the case for the OTS-coated silica surface, as supported by the TIRF data. Displacement of protein from an interface is a well studied phenomenon noted in several studies, and termed orogenic displacement by Mackie et al. (1999),[36] to describe compression of an adsorbed protein layer via surfactant adsorption at nucleation sites until a critical point in the surface pressure is reached, causing protein desorption. Since mAb-1 desorption appeared to be immediate on injection of polysorbate, the kinetics of polysorbate adsorption and displacement must be very rapid. The only case of slow mAb-1 desorption was for Tween 80 below its CMC, which could simply be a consequence of the concentration being 10-fold less than that for Tween 20 (compare the CMCs of Tween and 20 and 80). Under the dynamic condition of flow, polysorbate molecules can be envisaged to be continually "arriving" at the surface (since free surfactant molecules in bulk solution are thermodynamically unfavorable); therefore absolute concentration appears to be more relevant that concentration with respect to the CMC. Although polysorbate molecules self-assembled as a micelle above the CMC are thermodynamically stable, the micelle is a dynamic structure requiring consideration of lateral diffusion and exchange between free/assembled surfactant molecules. Evidence for the dynamic nature of a Tween 80 micelle has recently been provided by in silico modeling data.[37] Not all mAb-1 was washed off the surface following injection of Tween 20/80 above/below the CMC, which would suggest heterogeneity in the adsorbed protein population.

Residual adsorbed antibody has been observed following surfactant-induced displacement previously for both hydrophilic[38] and hydrophobic surfaces,[39] with the suggestion that protein adsorbed to the surface is irreversibly bound while subsequent adsorbed layers are reversibly bound. Oom et al. studied the adsorption of a hydrophilic and hydrophobic mAb, acquiring data showing surface loadings very similar to the results acquired here: ~5 and 10 mg/m^2 to bare silica, and ~2 mg/m^2 and negligible loading to bare silica in the presence of Tween 80, for the hydrophilic and hydrophobic mAb, respectively.[39] Interestingly, they were able to correlate differential adsorption behavior as a function of concentration up to 50 mg/mL, which is not possible to repeat by TIRF given the requirement to maintain transport limited diffusion. The presence of multiple layers of adsorbed mAb-1 to silica from pH 7.4 buffer is highly likely from consideration of the surface loading. Theoretical calculations of a packed antibody monolayer range from 1.3–2.7 mg/m^2 for dimensions of 146 × 135 × 69 Å, to 3.9 mg/m^2 for a sphere of 80 Å;[39] for both models these values are less than *ca.* 10 mg/m^2 measured for mAb-1 adsorbed to bare silica in these experiments. The expectation then is that a bilayer at least exists

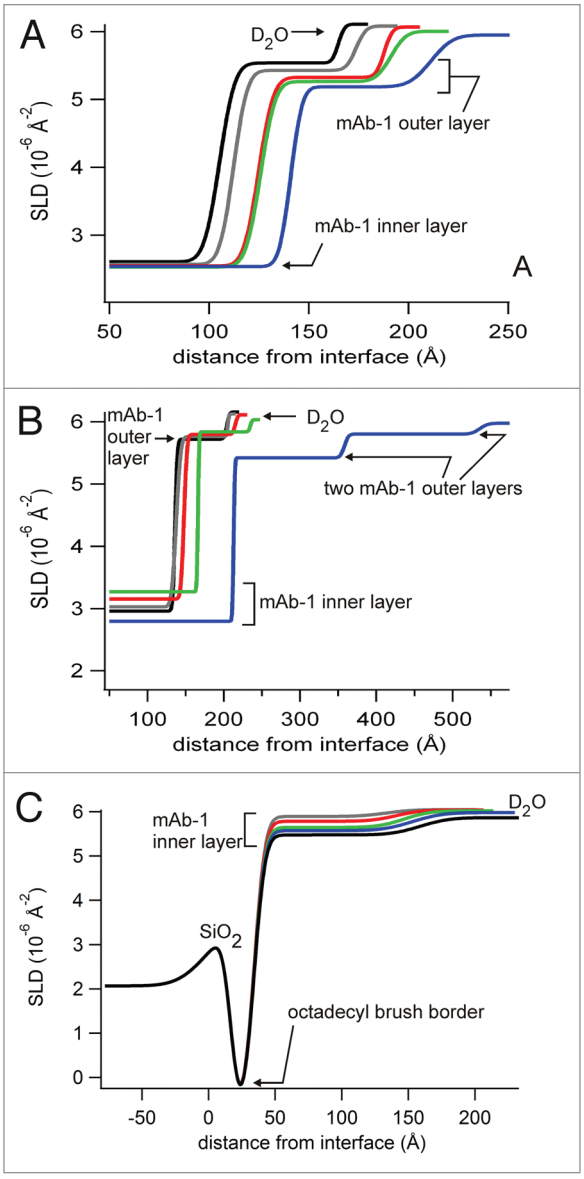

Figure 10. Fitted SLD profiles for neutron reflectivity data for mAb-1 adsorbed to SiO_2 from solutions in histidine pH 5.5 (A) or PBS pH 7.4 (B), and to OTS-coated SiO_2 from solutions in histidine pH 5.5 (C). Profiles are shown as the distance from the silicon-SiO_2 interface and labels are used as a guide for the SLD of each layer, corresponding to Table 1.

©2012 Landes Bioscience. Do not distribute.

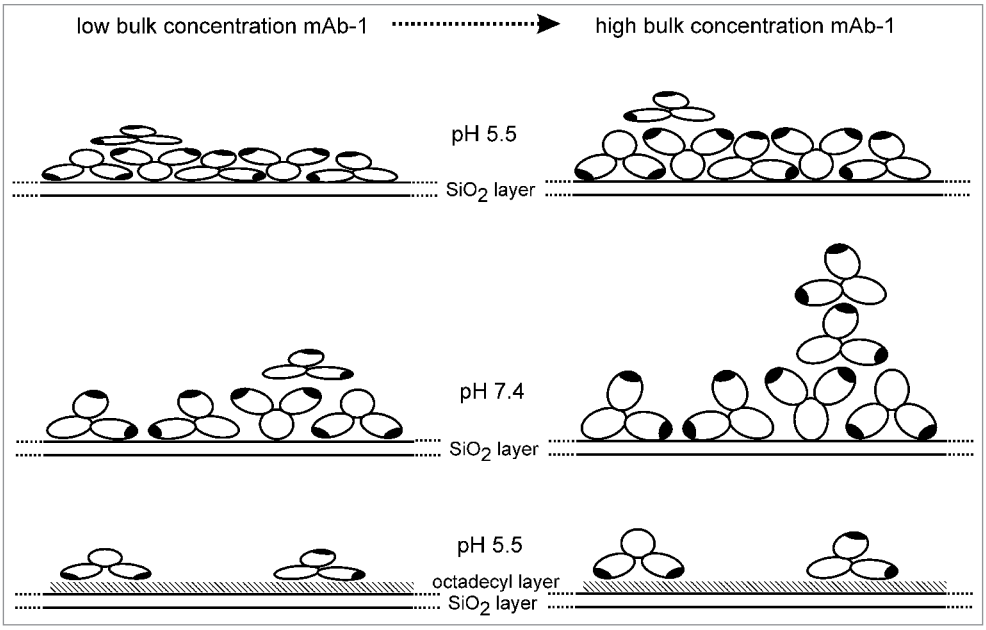

Figure 11. Cartoon of the change in surface fraction and molecular orientation (layer thickness) for the adsorption mAb-1 to SiO_2 and OTS-coated SiO_2 with increasing bulk concentration at pH 7.4 and 5.5.

Table 1. Fitted layer parameters for one-, two- and three-layer models of mAb-1 adsorbed to the SiO_2 and OTS-coated SiO_2 surface

Buffer and surface	mAb-1 conc. (mg/L)	*d*, inner layer* (Å)	*d*, outer layer§ (Å)	Protein fraction, inner layer	Protein fraction, outer layer§
pH 5.5, SiO_2 surface	50	95	60	0.99	0.22
	200	102	62	1.00	0.24
	500	115	63	1.00	0.27
	2000	117	66	1.01	0.29
	5000	130	70	1.01	0.31
pH 5.5, OTS-coated SiO_2 surface	50	99	n/a	0.12	n/a
	200	107	n/a	0.15	n/a
	500	113	n/a	0.19	n/a
	2000	119	n/a	0.21	n/a
	5000	125	n/a	0.23	n/a
pH 7.4, SiO_2 surface	50	131	68	0.89	0.17
	200	133	68	0.88	0.16
	500	141	67	0.84	0.15
	2000	160	69	0.81	0.14
	5000	207	145 *178*§	0.94	0.25 *0.15*§

d, layer thickness reported to the nearest whole number; *, the mAb-1 inner layer is in direct contact with the substrate; §, italicized numbers refer to the two outer layers seen for mAb-1 adsorbed to SiO_2 from 5000 mg/L solution, pH 7.4 only (trilayer model). The number of layers generated in each model was statistically verified by N-Sigma analysis.

and further discussion of the suitability of such a model for the experiments here is made against interpretation of neutron reflectivity data, below.

TIRF data for co-injection of polysorbate and mAb-1 to the surface also point to the importance of considering the dynamic of polysorbate micelles under conditions of flow. Above the CMC, the 2-fold increase in mAb-1 surface coverage observed (Fig. 4) may initially be surprising since a higher concentration of surfactant would be expected to compete more strongly for the surface. The explanation for this may be that, upon co-injection of mAb-1 with Tween 20 above its CMC, the surfactant saturates both the surface and non-specific binding sites on mAb-1,

©2012 Landes Bioscience. Do not distribute.

which remains natively folded. The retention of the native fold of mAb-1 is also predicted by calorimetry data for polysorbate interaction with a recombinant human IgG1.[40] In this scenario, the mAb-1/polysorbate complex approaches a surface also saturated with polysorbate. Resultant self-assembly of polysorbate chains at the silica and mAb-1 surfaces may therefore be driving the observed increase in mAb-1 surface coverage through either a change in protein packing or multiple protein layers; both models being observed by TIRF as simply an increase in the surface fraction of adsorbed protein. In contrast, TIRF data for co-injection of mAb-1 with polysorbate below the CMC suggest that the polysorbate molecules have a greater affinity for the silica surface than mAb-1 and ultimately attenuate adsorption. The affinity of the polysorbate molecules for the silica surface is therefore greater than their affinity for the mAb-1 surface and may reflect the interaction of the silica surface hydroxyl groups with the hydrophilic polysorbate polyethylene glycol (PEG) head groups. The transient peaks seen at the point of co-injection (Fig. 4) point to competition for the silica surface between free mAb-1 and free polysorbate molecules. The latter clearly out compete the mAb-1 molecules, most likely as a consequence of the smaller diffusion coefficient, which is five-orders of magnitude different (1.8×10^{-6} cm^2/s calculated for Tween 80,[37] vs. 1.99×10^{-11} cm^2/s for mAb-1 calculated by the Stokes-Einstein equation for a particle with measured hydrodynamic radius of 12.17 nm).

Pre-coating of the silica surface with polysorbate is expected to result in a change in surface functional groups exposed to the mAb-1 solution. Non-specific adsorption of Tween 20/80 to the silica surface is not expected to form a well defined PEGylated "brush border," as observed for self-assembled monolayers of very short chain PEGs for example.[41] The exposed surface functionality is, however, expected to be dominated by PEG, given the size of the Tween 20/80 head group (four PEG chains of n = 20) vs. the aliphatic tail of C12 (Tween 20) or $C18_{(9=9)}$ (Tween 80). Therefore, is it difficult to compare the surfaces in these experiments with densely packed tri(ethylene glycol) brush borders, which have been shown to repel protein.[41] It should not be assumed then that the surfaces pre-coated with Tween will rebuff mAb-1 adsorption. Rather, the increase of mAb-1 adsorption to pre-coated surfaces over the bare silica surfaces is consistent with work showing that surfaces of PEG of similar size (2000 MW) facilitate protein adsorption via structural rearrangements in the PEG backbone,[42] also observed by others.[43] Sheth and Leckband[42] proposed that protein interacts with the ethylene oxide units buried within long chained PEG monolayer, which could equally be applied as an explanation of the data acquired here.

mAb-1 adsorption to hydrophobic surfaces and the effect of polysorbate. The adsorption of mAb-1 to hydrophobic (OTS-coated silica) surfaces was intended to mimic adsorption to plastics such as polypropylene/polystyrene, as may be encountered. It is well established that the driving force in protein adsorption to hydrophobic surfaces includes entropic effects through dehydration of the surface.[44] It was immediately clear from TIRF data that mAb-1 adsorption to hydrophobic surfaces was much reduced compared with (hydrophilic) silica surfaces: approaching 2 mg/m^2 compared with 5.5–12 mg/m^2, respectively (Fig. 6). The reduction in adsorption to hydrophilic surfaces is consistent with previous data for antibody adsorption to a wide range of surfaces of different wettabilities, including the observation of no antibody adsorption to polyvinylchloride surfaces.[45] The surface loading of 2 mg/m^2 seen in these TIRF studies is the same as the loading seen for lysozyme to hydrophobic silica surfaces, despite the obvious difference in the proteins' size and architecture.[22] Tween 20 and particularly Tween 80 showed strong adsorption to the OTS-coated silica, displacing ~50% of pre-adsorbed mAb-1, with the kinetics of desorption being much faster for Tween 80 than for Tween 20. Hydrophobic interaction between the alkyl tail of the polysorbate and the octadecyl monolayer would be expected to drive polysorbate adsorption, leaving the PEG chains exposed to buffer. Faster desorption of mAb-1 by Tween 80 could therefore be ascribed to the stronger affinity of the longer alkyl chain of Tween 80 for the octadecyl monolayer, since both Tweens would have very similar diffusion coefficients. Partial desorption of lysozyme from hydrophobic silica by increasing concentrations of Tween 80 has also been reported, with the authors' concluding that a "strong Tween-surface association is necessary to inhibit protein adsorption."[22]

For OTS-coated silica surfaces pre-coated with Tween 20/80 (Fig. 8), the increase in mAb-1 adsorption for pre-coating with Tween concentrations above the CMC indicated that the surface was likely more hydrophilic. This is consistent with a polysorbate-coated octadecyl monolayer. (mAb-1 association with PEG groups being entirely consistent with the TIRF data for pre-coated bare silica and the data of others,[42] as discussed above.) Since the surface loadings remained well below 10 mg/m^2, it is unlikely that a saturated PEG surface can be envisaged and it is also possible that mAb-1 desorbed bound polysorbate to regenerate the hydrophobic surface, an observation previously noted by others for lysozyme adsorption to silica pre-coated with Tween 80.[22] The slightly reduced mAb-1 adsorption for pre-coating concentrations below the CMC indicates a less favorable binding interaction. This probably represents several underlying factors, including a heterogeneous surface, desorption of Tween by mAb-1 and differential mAb-1 binding affinities to polysorbate-free vs. -coated surface sites. A final consideration explaining the lower surface loadings on the OTS-coated silica following surface adsorption is protein relaxation. This has been suggested to involve a two-step process, first, interaction of the protein surface with the interface with rapid kinetics (seconds) and, second, exposure of the protein hydrophobic core to the interface with much slower kinetics dependent on the nature of the interface and protein.[46] Thus, where relaxation is extensive and significant tertiary structure is lost, a much thinner adsorbed protein layer will result, which effectively reduces the surface loading via an increase in the adsorbed footprint.

Characterizing mAb-1 adsorption to surfaces at the molecular level. Adsorption of mAb-1 from mildly acidic buffer pH 5.5 was less than that observed by TIRF at pH 7.4, to ~5.5 mg/m^2. A higher surface adsorption from pH nearer the protein pI is consistent with other reports.[47,48] For example, Wang et al. showed maximal adsorption for a mAb at a pH equivalent to its pI of 6 (> 3 mg/m^2), with a fall in adsorption to ~2.5 mg/m^2 at pH 4 and

©2012 Landes Bioscience. Do not distribute.

< 1mg/m^2 at pH 8.[48] Although the negative potential of silica is known to vary with pH,[49] we assumed these changes to be small (from pH 7 to 12 the zeta potential of silica varies between -60 and -70 mV), i.e., electrostatic interactions between mAb-1 at pH 7.4 and 5.5 and SiO_2 (silica) surface are expected to predominate.[31] The NR experiments, however, suggested more complex behavior for mAb-1 adsorption as a function of pH and concentration. For concentrations below 2000 mg/L, the bilayers (**Table 1**) fitted to the NR data showed that both inner and outer mAb-1 layers were noticeably thicker for adsorption to SiO_2 from pH 7.4, but the surface fractions were slightly less.

The differences in the SLD and layer thickness profiles (Fig. 10) can be explained by modeling two different orientations of adsorbed mAb-1 from pH 7.4 and 5.5. While no 3-D structure of mAb-1 exists, X-ray crystallography structures for other mAbs suggest the dimensions for a human IgG1 lie between 142 × 85 × 38 Å[50] and 146 × 135 × 69 Å.[51] At pH 5.5 and a bulk concentration of 50 mg/L, mAb-1 can therefore be assumed to be adsorbed to the SiO_2 surface (the inner layer) with an orientation lying between "side-on" (the smallest dimensions in the crystal structures) and "end-on" (the largest dimensions). As bulk concentration increases and the protein surface fraction remained very near saturation, adsorbed mAb-1 molecules at the SiO_2 surface tilted to an end-on position to accommodate further adsorbed molecules. In contrast, in pH 7.4 buffer, the orientation of mAb-1 adsorbed to the SiO_2 surface was near end-on for all concentrations below 2000 mg/L. This would suggest localized repulsion from the silica surface as regions rich in acidic residues gained negative potential as the buffer pH moved further from the pK_a of Asp/Glu side chains (pK_a 3.9–4.3). The positive potential of regions rich in basic residues would unlikely have changed much given that both buffer pH values are > 2 units from the pK_a of Lys/Arg side chains (pK_a 11.1–12.0). Therefore, the shift toward the pI of mAb-1 may be expected to reduce net electrostatic interaction with the silica surface, which was observed as a small decrease in the protein surface fraction. There is then an apparent disparity between the protein surface fractions calculated from NR data at pH 7.4 and 5.5, and the decrease in mAb-1 adsorption seen by TIRF at pH 7.4 and 5.5. This may be explained by an acid sensitivity of the Alex Fluor 488 dye during TIRF experiments at pH 5.5 as mentioned above, or consideration that end-on oriented mAbs have a smaller footprint such that the number of molecules adsorbed per unit area at both pH may not be that dissimilar.

For both pH values and concentrations up to 2000 mg/L, the adsorbed outer layer showed very little change, remaining tilted close toward a fully side-end orientation and with a much lower (sparse) protein surface fraction. The outer layer at the maximal concentration tested (5000 mg/L) at pH 7.4 showed a distinct behavior, whereas the change in moving from 2000 to 5000 mg/L at pH 5.5 continued the general trend of increasing layer thickness and protein surface fraction. At pH 7.4 the formation of a second outer layer and marked increase in the thickness of all three mAb-1 layers was observed. The thickness of the inner layer (mAb-1 adsorbed to the SiO_2 surface) was greater than should be possible from crystal structure coordinates, but it is unlikely that mAb-1 unfolded on increasing bulk surface concentration. Unfolded protein would not be well hydrated, nor extend into the aqueous buffer, instead forming a thin, spread layer as observed for denatured lysozyme at a hydrophobic surface.[34] Unfolding as a consequence of protein relaxation at the surface would also be envisaged to have the same outcome.

The model proposed here is one in which mAb-1 begins to adsorb from solution in oligomers, explaining the formation of a sparse third layer above an intermediate layer also of low surface fraction. The NR contrast between three protein layers where the outer two layers suggest the presence of sparse clusters is naturally relatively poor and for this reason it is likely that the fit to the data are less certain. For this reason, it is possible that the model-incorporated layers that appear to be thicker than would be envisaged for a mAb adsorbed end-on. It is important to note that there is good precedent for the observed behavior of mAb adsorption in discrete clusters, first from the general understanding that mAbs have a tendency to form oligomers (soluble aggregates) at higher concentrations[52] and second from atomic force microscopy images showing heterogeneous surface aggregates for a murine mAb at the silica surface.[19] Xu et al. also used NR to demonstrate that the murine mAb adsorbed to silica was not unfolded and tilted away from side-on orientations in a three-layer model at higher concentrations, consistent with this work. It is interesting that over the concentration range tested, we did not observe an adsorption process analogous to the surface pressure area isotherm of surfactants, as has previously been proposed for a IgG-like domain pair.[53] Even at the lowest concentration of 50 mg/L, the inner mAb layer had already approached saturation. Given that the protein surface fraction approached saturation, at least for the inner mAb-1 layer, it is inevitable that intermolecular interactions will have played a role in the packing density and orientation adopted.

mAb-1 adsorbed to hydrophobic (OTS-coated silica) surfaces as a sparse monolayer with a layer thickness indicating an orientation toward side-on at the lower concentrations tested, but tending toward fully end-on as the protein surface fraction increased. The absence of a thin, adsorbed layer with high surface fraction against the surface, as observed for lysozyme unfolding at an OTS-coated silica surface,[34] argues against unfolding of mAb-1. Maintenance of the native mAb-1 structure would predict minimal interaction between the hydrophilic/charged mAb-1 surface and octadecyl monolayer, consistent with the sparse layer observed. The non-uniformity of the layer may also point to the adsorption of oligomers, as discussed above. Recent quartz crystal microbalance data for a monoclonal human IgG1 adsorbed to a hydrophobic (dodecyl) self-assembled monolayer also showed side-on antibody orientation at low surface fractions, with transition to end-on orientation at higher surface fractions.[18] An end-on orientation wherein the Fc domains interact with the hydrophobic surface has been postulated following papain digestion of human IgG adsorbed to a hydrophobic surface with consequent release of the F_{ab}.[54] However, extrapolating such a model to mAb-1 would require further in-depth understanding of the role of local surface charge and exposed hydrophobic surface patches. For this reason, the adsorbed mAb-1 molecules in the

©2012 Landes Bioscience. Do not distribute.

cartoon summarizing the NR data (Fig. 11) have been shown in various random orientations.

To conclude, the adsorption of a human IgG to hydrophilic silica from pH 7.4 and 5.5 buffer and to hydrophobic OTS-coated silica from pH 5.5 was studied and interpreted through changes in surface loading of the adsorbed layer(s) and antibody orientation. We show that the relative abilities of Tween 20 and Tween 80 to desorb mAb from a hydrophilic or hydrophobic surface were dependent on the affinity of the polysorbate for the same surface. Following injection of polysorbate, a fraction of adsorbed mAb remained irreversibly bound to the surface and may represent multilayer systems with irreversibly and reversibly adsorbed layers. The polysorbate concentration and point at which it was introduced into the system was also critical. Conditions involving pre-coating of the glass surface with polysorbate above its CMC or simultaneous addition of polysorbate and mAb did not attenuate subsequent mAb adsorption to glass. Although the main criteria for addition of polysorbate to mAb formulation buffers is the stabilization of the monomeric state (i.e., prevention of aggregates, particularly under shear conditions), our data highlight the secondary effect of control of surface adsorption. mAb-1 clearly adsorbed less to hydrophobic surfaces than hydrophilic surfaces, and did not show evidence of unfolding over the time of the experiments. While a reduction in surface loading was observed for mAb-1 at pH 5.5 (further away from the pI of 8.99) by TIRF, the NR data suggested that the underlying molecular arrangement was more complex. Extensive reorientation of mAb-1 in contact with the silica surface occurred with change in pH. At pH 7.4, a fully end-on orientation was favored, with adsorption of mAb-1 at the highest concentration tested appearing to occur via soluble oligomers to generate the observed non-uniform triple layer.

Materials and Methods

Materials. Polysorbate 20 (Tween® 20), polysorbate 80 (Tween® 80), concentrated sulfuric acid (96–98%), dimethylsulfoxide (DMSO), toluene, *N,N*-dimethylformamide, OTS, potassium dichromate, sodium chloride, potassium chloride, sodium phosphate monobasic, potassium phosphate monobasic, sodium hydroxide, fluorescein isothiocyanate I (FITC), l-histidine monohydrochloride, sodium acetate, acetic acid, diiodomethane, 1,2-ethanediol (ethylene glycol), BSA and deuterium oxide (D_2O) were obtained from Sigma Aldrich at analytical grade or equivalent. Decon 90 was obtained from Decon Laboratories Limited, Hove, UK. Water was purified to > 14 MΩ.cm with a BioSelect (Purite, Oxon, UK). Alexa Fluor® 488 5-SDP ester (Alexa Fluor 488 sulfodichlorophenol ester) was purchased from Life Technologies Ltd (Invitrogen, Paisley, UK). The human monoclonal antibody (termed mAb-1) was kindly provided by MedImmune Ltd.

Fluorescent labeling of the mAb-1. Fluorescein isothiocyantate I (FITC) labeled mAb-1 was prepared following the manufacturer's instructions with minor modifications. FITC was dissolved in DMSO at 1 mg/mL and 100 μL slowly added under stirring to 3 mL of 20 mg/mL mAb-1 in phosphate buffered saline pH 7.4 (PBS), and left stirring in the dark for 2 h at room temperature. Unbound FITC was removed through extensive dialysis against PBS and the labeling ratio and protein concentration calculated using absorbance values at 280 and 495 nm. mAb-1 was labeled with Alexa Fluor 488 by addition of 1 mg Alexa Fluor 488 5-SDP ester to 1.5 mL mAb-1 dissolved in PBS to 50 mg/mL, and rotated at room temperature for 1 h to ensure thorough mixing. Unbound Alexa Fluor 488 5-SDP ester was removed through dialysis against l-histidine pH 5.5 at 4°C in the dark. The concentration of mAb-1 and the label:protein ratio were calculated using absorbance values at 280 and 494 nm according to the manufacturer's instructions.

Calculation of the diffusion coefficient of the mAb-1. The hydrodynamic diameter of mAb-1 at a concentration of 1 mg/mL in PBS was determined using dynamic light scattering (NanoZS). From the measured hydrodynamic diameter of mAb-1, the corresponding diffusion coefficient was calculated using the Stokes-Einstein Equation 2:

$$D = \frac{kT}{6\pi\eta r} \quad (2)$$

where D = diffusion coefficient; k = Boltzmann constant (1.381×10^{-23} m^2 kg s^{-2} K^{-1}); T = absolute temperature (Kelvin); r = hydrodynamic diameter (nm) and; η = viscosity of water at 25°C (0.89 centipoise).

Isothermal Calorimetry (ITC). BSA and mAb-1 were dialyzed using a Slide-a-Lyzer® dialysis cassette, 10,000 Dalton molecular weight cut-off, (Pierce, Thermo Scientific) overnight in 10 mM phosphate buffer pH 7.4. To ensure an exact buffer match, the dialyzed buffer was then used to prepare the Tween® 20 and Tween® 80 solutions. A VP-ITC (MicroCal™ Inc.) was used to carry out the calorimetric titration experiments. The titration experiments were undertaken at 25°C. Prior to each experiment, the sample cell and syringe were washed with 10% Decon 90 followed by distilled water and then 10 mM phosphate buffer. The reference cell was filled with degassed buffer. The reaction cell (volume 1.4 mL) was filled with the protein solution at a concentration of 14.4 mg/mL. The injection syringe, with a volume of 300 μL, was filled with surfactant solution in 10 mM phosphate buffer. The time delay prior to the first injection was 60 sec and the reference power was set to 10 μcal/s and the filter to 2 sec. Each titration experiment consisted of one injection of 1 μL followed by 25 injections with a volume of 10 μL. An injection speed of 0.5 μL/s was used for all injections with spacings of 300 sec between each injection. The time spacing between injections was set to a duration sufficient to allow the heat signal to return to the baseline. The paddle at the tip of the syringe was rotated at 300 rpm throughout the experiments. Titration experiments of surfactant into protein solution and control experiments of surfactant into buffer were performed using the same parameters. The titration curves were analyzed using Microcal's ORIGIN® software. The control titration experiments of surfactant into buffer were subtracted from surfactant into protein solution prior to fitting of the binding model. A one-site binding model was used to fit the data. The first injection, of 1 μL, was discarded from the data analysis.

©2012 Landes Bioscience. Do not distribute.

Total internal reflection fluorescence (TIRF). Quartz (silica) slides were cleaned by immersion in chromic acid (80 g $K_2Cr_2O_7$ per liter 96–98% sulfuric acid) for 1 h, followed by thorough rinsing with deionized water. Slides were left in deionized water overnight and then dried. Hydrophobized silica slides were prepared by immersion in a solution of 0.14 g octadecyltrichlorosilane (OTS) in 180 mL of n-hexadecane for 2 h under stirring at room temperature, as described by Pereira et al.[55] The width of the flow chamber, 1.6 cm, and the gasket thickness, 0.01 cm, of the TIRF cell were maintained throughout (TIRF Flow System, TIRF Technologies Inc.), and fluorescence measured using a Varian Cary Eclipse spectrofluorometer (Agilent Technologies). Blank runs of FITC in PBS, Alexa Fluor 488 5-SDP in l-histidine pH 5.5, and unlabeled mAb-1 in PBS were performed to verify that their contribution to the fluorescence signal was negligible. Calibration of the raw fluorescence data was acquired previously for an immunoglobulin domain pair known to adsorb almost irreversibly to bare silica at surface saturation[55] and characterized against neutron reflectivity data for the same protein.[53] That is, for a series of bulk concentrations of the domain pair introduced into the TIRF cell, the fluorescence signal at steady-state following adsorption and buffer rinse was calibrated against the fitted neutron reflectivity data for the adsorbed domain pair following the same concentration range and buffer rinse of the cell. With the same TIRF set-up in these experiments, fluorescence units were converted to surface coverage, albeit for a non-identical but related immunoglobulin protein.

Confirmation of transport-limited adsorption of mAb-1 to the surface was made by changing the shear rate and concentration of mAb-1 while measuring the change in fluorescence. Shear rates from 6 to 84 sec^{-1} were controlled using a syringe pump driver (KD Scientific). A shear rate of 6 sec^{-1} was found to produce reproducible adsorption profiles for mAb-1 over concentrations from 5 to 50 mg/L in PBS. The effect of surfactant on mAb-1 surface adsorption to silica was investigated at both pH 5.5, using the largely acid-insensitive Alexa Fluor 488 label (λ_{ex} 495 nm, λ_{em} 519 nm), and pH 7.4 using the fluorescein label (λ_{ex} 450 nm, λ_{em} 520 nm). The effects of Tween 20 at concentrations of 0.05 and 1 mM (CMC in water ~80 μM), and Tween 80 at concentration of 5 μM and 1 mM (CMC in water ~12 μM) were studied under three conditions: 1) co-dissolved with mAb-1; 2) injection into the flow chamber (over 1800 sec) before mAb-1 injection (over 3600 sec); and 3) injection into the flow chamber (over 1800 sec) after mAb-1 injection (over 1800 sec). The same set of experiments was undertaken at pH 5.5 using an OTS-coated silica surface to investigate mAb-1 surface adsorption to a hydrophobic surface. In all cases, the adsorption/desorption profiles shown in the figures are each an average from five individual experiments run under the same conditions.

Neutron reflectometry. Silicon < 111 > substrates 10 cm in diameter and with a thickness of 1 cm were washed with Decon 90, thoroughly rinsed with deionized water and dried under a nitrogen stream. The hydrophobic silicon wafer was prepared by immersion in a 1 mM solution of OTS in *n*-hexadecane for 2 h to allow self-assembly of the silane monolayer.[56] The surface was thoroughly rinsed with dichloromethane, ethanol and water, sequentially. The cleaned silicon substrate was then clamped to a silicon trough with a void volume of *ca*. 3 mL. The experiments were performed at mAb-1 concentrations from 50 to 5000 mg/L in acetate buffer pH 5.5 and phosphate buffer 7.4 for the silicon surface, and at pH 5.5 for the OTS-coated silicon surface. The neutron reflectometry experiments were undertaken using the INTER instrument at ISIS (Rutherford Appleton Laboratory). The sample was analyzed at fixed incident angles of 0.7 and 2.3°, with the data reduced to yield a single reflectivity profile with Q values up to 0.3 $Å^{-1}$. The wavelength of the neutrons used ranged from 1.0 to 15.0 Å. A flat background, determined by extrapolation to high values of momentum transfer Q ($Q = 4\pi\sin\theta/\lambda$, where θ is the glancing angle of incidence and λ the wavelength) was subtracted. All the experiments were conducted at 25°C. Blank substrate/buffer measurements were performed for substrate characterization. Following adsorption of protein to the SiO_2/OTS-coated SiO_2 surface for 30 min, surfaces were rinsed by flushing the trough with five (trough) volumes of buffer-H_2O or buffer-D_2O as appropriate to investigate the extent of protein desorption.

Fitting of the experimental data required a theoretical calculation of the SLD of mAb-1 in H_2O at pH 7. We used a spreadsheet method of Dr. R. May, Institut Laue-Langevin, which involved summing the scattering lengths for each amino acid. To calculate the SLD of mAb-1 in D_2O, an assumption of the fraction exchange of non-hydrogen bonded N-H protons must be made. We initially assumed a 70% exchange, in accordance with time course data for lysozyme adsorbed to silica (SiO_2) particles.[33] No calculation of H/D exchange based on a known hydrogen bonding pattern could be made since the 3-dimensional structure for mAb-1 has not been determined. Equation 3 was used to calculate the protein fraction of the layer covering a surface (*a*) from the fitted SLD (ρ) made up from contributions of the protein and subphase.

$$r_{fitted} = (1 - a).r_{D_2O} + a.r_{calc}$$

NR data were fitted using a Global MOTOFIT analysis.[57] First, parameters for the cleaned surfaces measured against D_2O were obtained. These parameters were kept fixed for subsequent fits of the adsorbed protein layers. This ensured that changes between subsequent protein adsorption steps were recorded in the protein layers only. Layer thicknesses are reported to the nearest whole number. The SLD value for the silicon substrate was constrained to 2.07×10^{-6} $Å^{-2}$. The SLDs for H_2O and D_2O were allowed to migrate 5% from nominal values of -0.56 and 6.36 ($\times 10^{-6}$ $Å^{-2}$), respectively. Backgrounds ranged between $5.0–6.0 \times 10^{-6}$ $Å^{-2}$ for bare SiO_2 and ~3.0×10^{-6} $Å^{-2}$ for OTS-coated SiO_2, and were included as a fitting parameter. The thickness for the SiO_2 layer for the two bare substrates was 3 and 7 Å, with the SLDs constrained to 3.47×10^{-6} $Å^{-2}$. For the OTS-coated substrate, the SiO_2 layer was 17 Å with a SLD of 3.55×10^{-6} $Å^{-2}$, reflecting a thicker and more porous oxide layer. Surface roughnesses against silicon and SiO_2 ranged between 2–11 Å, with higher roughnesses fitted for layers interfaced against a protein layer (generally 4–7 Å). To test the validity of the models fitted to

©2012 Landes Bioscience. Do not distribute.

the data, particularly where two models with differing layer numbers could be plausibly proposed, we undertook N-Sigma analysis to weight the χ^2 value for each model against the number of data points and number of parameters.[35] When comparing two models, the parameters for the Si/SiO_2 layers were fixed for both, such that the number of free parameters was three for a one-layer model and six for a two-layer model.

Contact angle goniometry (CAG) and surface energy determination. Microscope coverslips 13 mm in diameter were coated with 1 mM OTS using a previously established method.[58] The liquid-surface interactions were investigated by determination of the contact angles of small drops (5 per liquid) of filtered water, diiodomethane and 1,2-ethanediol on silica, OTS-coated silica and Tween coated OTS substrates using a goniometer (Krüss DSA30B, Hamburg, Germany). Surface energies of the substrates (γ_s) were calculated from the contact angles and interfacial energies of the three probe liquids using an in-house Visual Basic program.[58,59]

Disclosure of Potential Conflicts of Interest

No potential conflicts of interest were disclosed.

Acknowledgments

R.G.C. is the recipient of a doctoral training scholarship from MedImmune Ltd. The NR beam-time at ISIS was funded by the Science and Technology Facilities Council, experiment number RB1120015.

References

1. Elvin JG, Couston RG, van der Walle CF. Therapeutic antibodies: Market considerations, disease targets and bioprocessing. Int J Pharm 2011; In press; PMID:22227342.
2. Ripple DC, Dimitrova MN. Protein particles: What we know and what we do not know. J Pharm Sci 2012; 101:3568-79; PMID:22736521.
3. Pinholt C, Hartvig RA, Medlicott NJ, Jorgensen L. The importance of interfaces in protein drug delivery - why is protein adsorption of interest in pharmaceutical formulations? Expert Opin Drug Deliv 2011; 8:949-64; PMID:21557707.
4. Bee JS, Randolph TW, Carpenter JF, Bishop SM, Dimitrova MN. Effects of surfaces and leachables on the stability of biopharmaceuticals. J Pharm Sci 2011; 100:4158-70; PMID:21523787.
5. Bee JS, Chiu D, Sawicki S, Stevenson JL, Chatterjee K, Freund E, et al. Monoclonal antibody interactions with micro- and nanoparticles: adsorption, aggregation, and accelerated stress studies. J Pharm Sci 2009; 98:3218-38; PMID:19492408.
6. Bee JS, Goletz TJ, Ragheb JA. The future of protein particle characterization and understanding its potential to diminish the immunogenicity of biopharmaceuticals: A shared perspective. J Pharm Sci 2012; 101:3580-5; PMID:22736570.
7. Johnson R, Jiskoot W. Models for evaluation of relative immunogenic potential of protein particles in biopharmaceutical protein formulations. J Pharm Sci 2012; 101:3586-92; PMID:22736238.
8. Singh SK. Impact of product-related factors on immunogenicity of biotherapeutics. J Pharm Sci 2011; 100:354-87; PMID:20740683.
9. Ohtake S, Kita Y, Arakawa T. Interactions of formulation excipients with proteins in solution and in the dried state. Adv Drug Deliv Rev 2011; 63:1053-73; PMID:21756953.
10. Maity H, Karkaria C, Davagnino J. Effects of pH and arginine on the solubility and stability of a therapeutic protein (Fibroblast Growth Factor 20): relationship between solubility and stability. Curr Pharm Biotechnol 2009; 10:609-25; PMID:19619121.
11. Maa YF, Hsu CC. Protein denaturation by combined effect of shear and air-liquid interface. Biotechnol Bioeng 1997; 54:503-12; PMID:18636406.
12. Kiese S, Papppenberger A, Friess W, Mahler HC. Shaken, not stirred: mechanical stress testing of an IgG1 antibody. J Pharm Sci 2008; 97:4347-66; PMID:18240293.
13. Krägel J, Wustneck R, Clark D, Wilde P, Miller R. Dynamic surface-tension and surface shear rheology studies of mixed beta-lactoglobulin tween-20 systems. Colloid Surf. A-Physicochem. Eng. Asp. 1995; 98:127-35.
14. Kreilgaard L, Jones LS, Randolph TW, Frokjaer S, Flink JM, Manning MC, et al. Effect of Tween 20 on freeze-thawing- and agitation-induced aggregation of recombinant human factor XIII. J Pharm Sci 1998; 87:1597-603; PMID:10189273.
15. McLeod AG, Walker IR, Zheng S, Hayward CPM. Loss of factor VIII activity during storage in PVC containers due to adsorption. Haemophilia 2000; 6:89-92; PMID:10781194.
16. Mathes J, Friess W. Influence of pH and ionic strength on IgG adsorption to vials. Eur J Pharm Biopharm 2011; 78:239-47; PMID:21421047.
17. Santore MM, Wertz CF. Protein spreading kinetics at liquid-solid interfaces via an adsorption probe method. Langmuir 2005; 21:10172-8; PMID:16229542.
18. Wiseman ME, Frank CW. Antibody adsorption and orientation on hydrophobic surfaces. Langmuir 2012; 28:1765-74; PMID:22181558.
19. Xu H, Zhao XB, Grant C, Lu JR, Williams DE, Penfold J. Orientation of a monoclonal antibody adsorbed at the solid/solution interface: a combined study using atomic force microscopy and neutron reflectivity. Langmuir 2006; 22:6313-20; PMID:16800692.
20. Mackie AR, Gunning AP, Ridout MJ, Wilde PJ, Rodriguez Patino J. In situ measurement of the displacement of protein films from the air/water interface by surfactant. Biomacromolecules 2001; 2:1001-6; PMID:11710002.
21. Woodward NC, Gunning AP, Maldonado-Valderrama J, Wilde PJ, Morris VJ. Probing the in situ competitive displacement of protein by nonionic surfactant using atomic force microscopy. Langmuir 2010; 26:12560-6; PMID:20608707.
22. Joshi O, McGuire J. Adsorption behavior of lysozyme and Tween 80 at hydrophilic and hydrophobic silica-water interfaces. Appl Biochem Biotechnol 2009; 152:235-48; PMID:18478369.
23. Wertz CF, Santore MM. Adsorption and relaxation kinetics of albumin and fibrinogen on hydrophobic surfaces: Single-species and competitive behavior. Langmuir 1999; 15:8884-94.
24. Wertz CF, Santore MM. Adsorption and reorientation kinetics of lysozyme on hydrophobic surfaces. Langmuir 2002; 18:1190-9.
25. Lassen B, Malmsten M. Competitive protein adsorption studied with TIRF and ellipsometry. J Colloid Interface Sci 1996; 179:470-7.
26. Lakey JH. Neutrons for biologists: a beginner's guide, or why you should consider using neutrons. J R Soc Interface 2009; 6(Suppl 5):S567-73; PMID:19656821.
27. Le Brun AP, Holt SA, Shah DSH, Majkrzak CF, Lakey JH. The structural orientation of antibody layers bound to engineered biosensor surfaces. Biomaterials 2011; 32:3303-11; PMID:21306769.
28. Garidel P, Hoffmann C, Blume A. A thermodynamic analysis of the binding interaction between polysorbate 20 and 80 with human serum albumins and immunoglobulins: a contribution to understand colloidal protein stabilisation. Biophys Chem 2009; 143:70-8; PMID:19427732.
29. Rebar VA, Santore MM. A total internal reflectance fluorescence nanoscale probe of interfacial potential and ion screening in polyethylene oxide layers adsorbed onto silica. J Colloid Interface Sci 1996; 178:29-41.
30. Fu ZG, Santore MM. Poly(ethylene oxide) adsorption onto chemically etched silicates by Brewster angle reflectivity. Colloids Surf A Physicochem Eng Asp 1998; 135:63-75.
31. Mathes J, Friess W. Influence of pH and ionic strength on IgG adsorption to vials. Eur J Pharm Biopharm 2011; 78:239-47; PMID:21421047.
32. McGovern ME, Kallury KMR, Thompson M. Role of solvent on the silanization of glass with octadecyltrichlorosilane. Langmuir 1994; 10:3607-14.
33. Larsericsdotter H, Oscarsson S, Buijs J. Thermodynamic analysis of lysozyme adsorbed to silica. J Colloid Interface Sci 2004; 276:261-8; PMID:15271551.
34. Lu JR, Su TJ, Thirtle PN, Thomas RK, Rennie AR, Cubitt R. The denaturation of lysozyme layers adsorbed at the hydrophobic solid/liquid surface studied by neutron reflection. J Colloid Interface Sci 1998; 206:212-23; PMID:9761646.
35. Ihringer J. A quantitative measure for the goodness of fit in profile refinements with more than 20 degrees of freedom. J Appl Cryst 1995; 28:618-9.
36. Mackie AR, Gunning AP, Wilde PJ, Morris VJ. Orogenic displacement of protein from the air/water interface by competitive adsorption. J Colloid Interface Sci 1999; 210:157-66; PMID:9924119.
37. Amani A, York P, de Waard H, Anwar J. Molecular dynamics simulation of a polysorbate 80 micelle in water. Soft Matter 2011; 7:2900-8.
38. You HX, Lowe CR. AFM studies of protein adsorption. 2. Characterization of immunoglobulin G adsorption by detergent washing. J Colloid Interface Sci 1996; 182:586-601.
39. Oom A, Poggi M, Wikström J, Sukumar M. Surface interactions of monoclonal antibodies characterized by quartz crystal microbalance with dissipation: impact of hydrophobicity and protein self-interactions. J Pharm Sci 2012; 101:519-29; PMID:21938730.
40. Hoffmann C, Blume A, Miller I, Garidel P. Insights into protein-polysorbate interactions analysed by means of isothermal titration and differential scanning calorimetry. Eur Biophys J 2009; 38:557-68; PMID:19189101.
41. Skoda MW, Schreiber F, Jacobs RM, Webster JR, Wolff M, Dahint R, et al. Protein density profile at the interface of water with oligo(ethylene glycol) self-assembled monolayers. Langmuir 2009; 25:4056-64; PMID:19714891.

©2012 Landes Bioscience. Do not distribute.

42. Sheth SR, Leckband D. Measurements of attractive forces between proteins and end-grafted poly(ethylene glycol) chains. Proc Natl Acad Sci U S A 1997; 94:8399-404; PMID:9237988.
43. Efremova NV, Sheth SR, Leckband DE. Protein-Induced Changes in Poly(ethylene glycol) Brushes:?Molecular Weight and Temperature Dependence. Langmuir 2001; 17:7628-36.
44. Duncan MR, Lee JM, Warchol MP. Influence of surfactants upon protein peptide adsorption to glass and polypropylene. Int J Pharm 1995; 120:179-88.
45. Zangmeister RA. Application of X-ray photoelectron spectroscopic analysis to protein adsorption on materials relevant to biomanufacturing. J Pharm Sci 2012; 101:1639-44; PMID:22227836.
46. Xu LC, Siedlecki CA. Effects of surface wettability and contact time on protein adhesion to biomaterial surfaces. Biomaterials 2007; 28:3273-83; PMID:17466368.
47. Buijs J. vandenBerg PAW, Lichtenbelt JWT, Norde W, Lyklema J. Adsorption dynamics of IgG and its F(ab')(2) and Fc fragments studied by reflectometry. J Colloid Interface Sci 1996; 178:594-605.
48. Wang XQ, Wang YN, Xu H, Shan HH, Lu JR. Dynamic adsorption of monoclonal antibody layers on hydrophilic silica surface: a combined study by spectroscopic ellipsometry and AFM. J Colloid Interface Sci 2008; 323:18-25; PMID:18452935.
49. Behrens SH, Grier DG. The charge of glass and silica surfaces. J Chem Phys 2001; 115:6716-21.
50. Silverton EW, Navia MA, Davies DR. Three-dimensional structure of an intact human immunoglobulin. Proc Natl Acad Sci U S A 1977; 74:5140-4; PMID:270751.
51. Harris LJ, Skaletsky E, McPherson A. Crystallographic structure of an intact IgG1 monoclonal antibody. J Mol Biol 1998; 275:861-72; PMID:9480774.
52. Kükrer B, Filipe V, van Duijn E, Kasper PT, Vreeken RJ, Heck AJ, et al. Mass spectrometric analysis of intact human monoclonal antibody aggregates fractionated by size-exclusion chromatography. Pharm Res 2010; 27:2197-204; PMID:20680668.
53. Kreiner M, Chillakuri CR, Pereira P, Fairhead M, Li Z, Mardon HJ, et al. Orientation and surface coverage of adsorbed fibronectin cell binding domains and bound integrin α5β1 receptors. Soft Matter 2009; 5:3954-62.
54. Yu DQ, Ghosh R. Method for studying immunoglobulin G binding on hydrophobic surfaces. Langmuir 2010; 26:924-9; PMID:20067307.
55. Pereira P, Kelly SM, Gellert PR, van der Walle CF. Interdomain mobility and conformational stability of type III fibronectin domain pairs control surface adsorption, desorption and unfolding. Colloids Surf B Biointerfaces 2008; 64:1-9; PMID:18261887.
56. Lu JR, Su TJ, Thirtle PN, Thomas RK, Rennie AR, Cubitt R. The denaturation of lysozyme layers adsorbed at the hydrophobic solid/lquid surface studied by neutron reflection. J Colloid Interface Sci 1998; 206:212-23; PMID:9761646.
57. Nelson A. Co-refinement of multiple-contrast neutron/X-ray reflectivity data using MOTOFIT. J Appl Cryst 2006; 39:273-6.
58. Lamprou DA, Smith JR, Nevell TG, Barbu E, Willis CR, Tsibouklis J. Towards the determination of surface energy at the nanoscale: a further assessment of the AFM-based approach. J Adv Microsc Res 2010; 5:137-42.
59. Lamprou DA, Smith JR, Nevell TG, Barbu E, Willis CR, Tsibouklis J. Self-assembled structures of alkanethiols on gold-coated cantilever tips and substrates for atomic force microscopy: Molecular organisation and conditions for reproducible deposition. Appl Surf Sci 2010; 256:1961-8.

©2012 Landes Bioscience. Do not distribute.